

# Calibration of WCDs for the Auger Observatory

J.C. D'Olivo<sup>1</sup>, A. Fernández<sup>2</sup>, O. Martínez<sup>2</sup>, M. Medina<sup>3</sup>, L. Nellen<sup>1</sup>, H. Salazar<sup>2</sup>, J.F. Valdés-Galicia<sup>4</sup>,  
L. Villaseñor<sup>3</sup>, and A. Zepeda<sup>5</sup>

<sup>1</sup>*Instituto de Ciencias Nucleares, UNAM, Apdo. Postal 70-543, 04510 México, D.F., México*

<sup>2</sup>*Facultad de Ciencias, BUAP, 72 000 Puebla, Pue., México*

<sup>3</sup>*Instituto de Física y Matemáticas, Universidad Michoacana de San Nicolás de Hidalgo, Apdo. Postal 2-82, Morelia, Mich., 58040, México*

<sup>4</sup>*Instituto de Geofísica, UNAM, 04510 México, D.F., México*

<sup>5</sup>*Departamento de Física, Cinvestav-IPN, 07000 México, D.F., México*

## Abstract

The large area covered by the surface detectors of the Pierre Auger Observatory requires efficient calibration and monitoring methods that can be used remotely. We present a way to calibrate and monitor the performance of the individual surface detector stations of the Auger Observatory. This method is based on the analysis of signals from crossing muons as well as signals from electrons produced in muon decays inside a water Čerenkov detector (WCD) prototype for the Auger Observatory. We discuss the different triggers that can be used to obtain these events and the on-line calibration and monitoring histograms along with the way these data can be used to diagnose component failures of any of the surface stations of the Auger Observatory. We also present detector simulation results that are in good agreement with the experimental data.

## 1 Introduction:

The main purpose of the Pierre Auger Observatory (PAO) is to study the origin and nature of the cosmic rays reaching the earth with energies above  $10^{19}$  eV and to measure their energy spectra, their arrival direction and their composition (Auger, 1997). These cosmic rays carry macroscopic energies on microscopic particles and their acceleration mechanism remains as one of the biggest and oldest mysteries in astrophysics. At these extreme energies, the cosmic rays are constrained by the GZK effect (Greisen, 1965; Zatsepin, G.T. and Kuz'min, V.A., 1966) to travel distances shorter than about 100 Mpc. As a consequence, their trajectories are deflected only a few degrees in the typical intergalactic magnetic fields of a few nanogauss. Therefore, their arrival direction provides important information about their source location in the sky. The Auger Observatory surface detector is described elsewhere (Auger Collaboration, 1997). For a surface array as big as this one ( $3000 \text{ km}^2$ ) it is indispensable that the continuous calibration and monitoring of each WCD can be done remotely. In the present paper we describe one way in which these tasks can be performed on the basis of the flux of secondary cosmic ray muons reaching the surface detectors. This flux is about  $250 \text{ muons/m}^2 \text{ s}$  at sea level and even higher at the Auger sites. Muons with energies greater than about 300 MeV cross the detector completely and in the process leave a Čerenkov signal which is, on the average, constant in time; lower-energy muons can stop and decay inside the water volume of the detectors, in the latter case, the decay electron will give rise to a Čerenkov signal which is also constant in time. These signals can be used on-line to provide an absolute calibration of the energy scale of the surface stations and to obtain a reliable way to monitor and diagnose the performance of each of the 1600 stations in a remote way.

## 2 Experimental Setup and Discussion:

The WCD prototype we used consisted of a full-sized prototype made of a polyethylene cylinder with a cross section of  $10 \text{ m}^2$  filled with purified water up to a height of 1.2 m; the tank had three 8" PMTs looking downwards at the tank volume from the water surface. The inner surface of the tank was covered with a highly reflective tyvek sheet (reflectivity of about 90% in the ultraviolet region of the EM spectrum) cut to the cylindrical shape and kept in place by circular PVC hoses tightly stretched against the inner walls of the tank.

It is useful to take the Čerenkov signal from muons that cross the detector vertically as a reference point; for this purpose we used the experimental setup shown in Figure 1. A 1" slab of steel was placed between the bottom of the tank and the lower hodoscope in order to harden the energy spectrum of the triggering muons. For the purpose of acquiring events in which the muons either cross the detector or stop and decay inside it we used the experimental setup shown in Figure 2.

The trigger for the first case (Figure 1), is simply given by the time coincidence of the PMT pulses from two scintillation hodoscopes placed vertically, one above and the other below the tank. The trigger for the second case (Figure 2) is given by the presence of an isolated signal (i.e., no further PMT activity in a time window of  $20 \mu\text{s}$ ) in the sum of the three PMTs above  $30 \text{ mV}$  or by the occurrence of two consecutive signals above  $30 \text{ mV}$  in the sum of the pulses from the three PMTs within a time window of  $20 \mu\text{s}$ , respectively. The CAMAC controller used was the LeCroy 8901; it was connected to a National Instruments GPIB port on a pentium PC running at  $133 \text{ MHz}$ . The DAQ program was written in LabView, a graphic programming package from National Instruments.

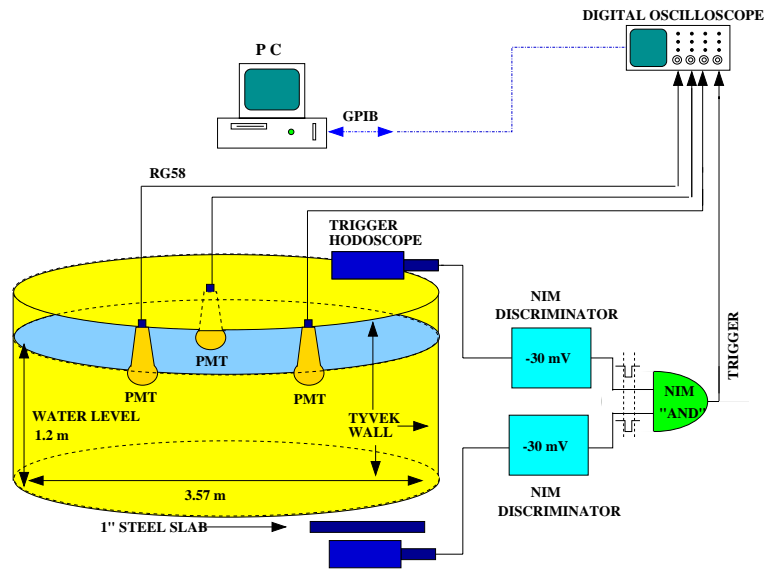


Figure 1: Schematic diagram of the experimental array used to collect events with muons that cross the detector vertically.

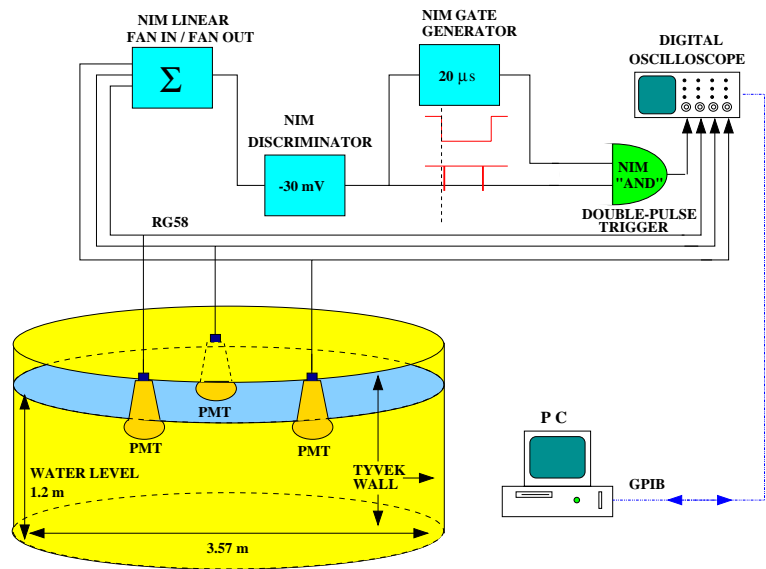


Figure 2: Schematic diagram of the experimental array used to collect events with muons that either stop and decay inside the detector, or cross it at any angle.

The calibration procedure using crossing muons on one hand and decay electrons on the other is described in detail elsewhere (Alarcon et al., 1999) for a tank of reduced dimensions with a single PMT; therein it is shown that detailed simulations are in good agreement with experimental data; in the case of full-sized WCDs with three PMTs the procedure is similar. Figure 3 shows clear peaks on the charge distributions for crossing muons as well as decay electrons. From simulations we expect for the full-size tank, taking the sum of the three PMTs, a signal of about 75% of that generated by a single PMT in the reduced prototype due to the lower ratio of the area of the three photocathodes to the cross wall area of the detector. To avoid problems due to the smaller signal, one can require double or triple coincidences on the PMTs, at the same time enhancing the signal to noise ratio. A potential problem which requires further study for the application of the decay-electron method is increase of

potential problem which requires further study for the application of the decay-electron method is increase of

random muon coincidences in the bigger tank.

**2.1 Triggers:** The following level-2 triggers will be used to calibrate and monitor the Auger WCDs remotely and continuously:

- 1) Isolated Muon. Defined as  $\text{Sum}(\text{Signals from PMTs}) > 15\% \text{ VEM}$  and no further PMT activity in  $20 \mu\text{s}$ , where 1 VEM is the signal corresponding to one vertical muon.
- 2) Double-Coincidence Isolated Muon. Defined as 1) and two PMTs in coincidence.
- 3) Triple-Coincidence Isolated Muon. Defined as 1) and three PMTs in coincidence.
- 4) Double-Pulse. Defined as two pulses in a time window of  $20 \mu\text{s}$  with variable threshold with  $\text{Sum}(\text{Signals from PMTs})$  for first pulse  $> th_1 \text{ VEM}$  and  $\text{Sum}(\text{Signals from PMTs})$  for second pulse  $> th_2 \text{ VEM}$ , where  $th_1$  and  $th_2$  will be of the order of 15% and will be optimized for muon-decay discrimination.
- 5) LED. Obtained by operating an LED flasher inside the detectors.

**2.2 Calibration Histograms:** A set of histograms will be used to obtain an absolute calibration of each station on the basis of the average energy deposition of through-going muons associated with Isolated-Muon events, and decay electrons associated with Double-Pulse events. The LED events will be used to calibrate the gains of the ADCs used for the the most significant bits of the dynamic range by comparing with overlapping bits of lower significance. The following histograms will be used for each case: Isolated Muons events (IM)

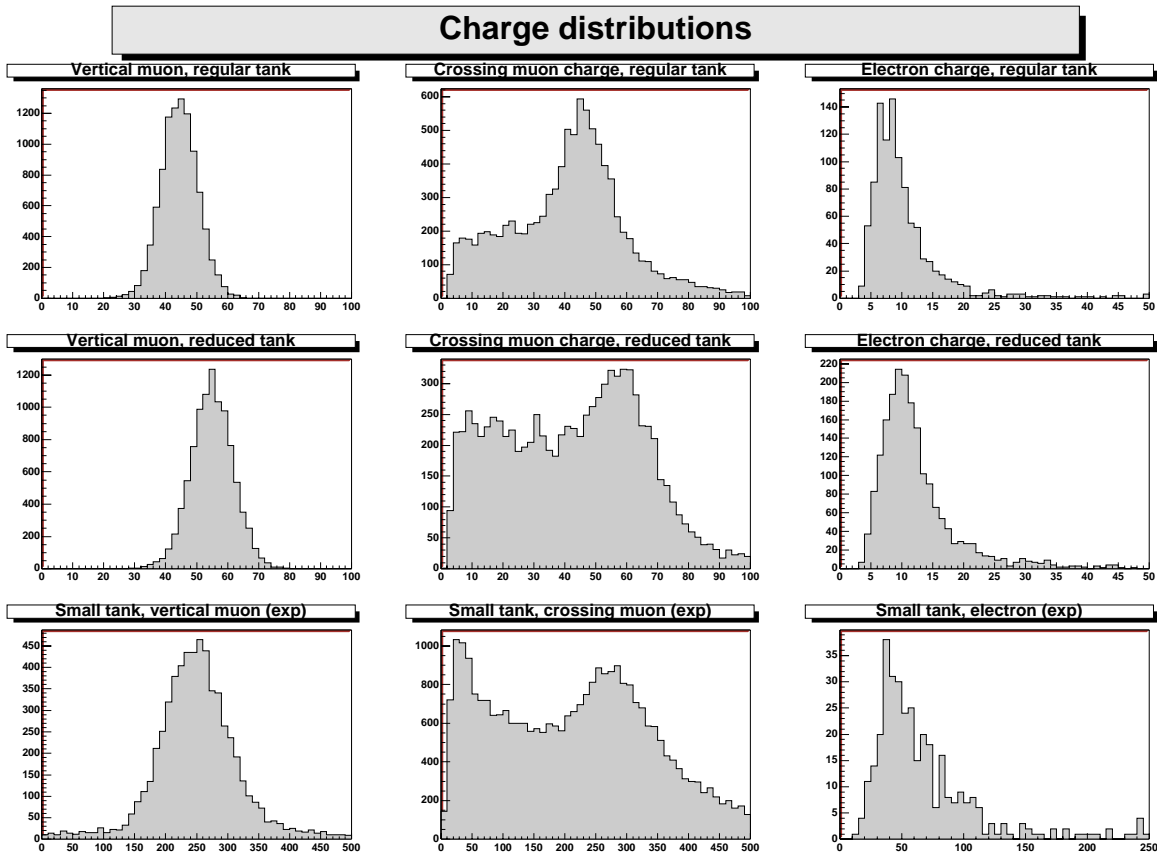


Figure 3: Charge distributions for vertical muons (column 1), crossing muons (column 2) and decay electrons (column 3). Experimental distributions (row 3) and simulation (row 2) for the reduced prototype show good agreement. Simulations for a full size tank (row 1) show somewhat smaller charges collected due to the relatively reduced photo cathode area.

$Q$ ,  $V$ .  $Q/V$  and event rate; LED events (LED)  $Q$ ,  $V$ , and  $Q/V$ ; Double-Pulse events (D-P)  $Q_1, V_1, Q_1/V_1$ , rate,  $Q_2, V_2, Q_2/V_2$ , and  $t_{12}$ .

**2.3 Monitoring Histograms:** In addition of the above, the following analogue sensors provide on-line information about performance and the operating conditions of each detector station:

At least the following 9 temperatures: Water, air inside tank, air outside tank, three PMTs, front-end electronics, batteries, tank top,

Voltage and current for each PMT,

Input current, output current and voltage for the solar panel,

Cloud detectors,

Pressure monitor at tank bottom to calculate water level,

Atmospheric pressure,

Others up to 32 channels.

**2.4 Diagnosis:** The following diagnoses will be done on-line on the basis of the monitoring data.

Failure: Dirty water. Signature:  $Q$ ,  $V$ , and  $Q/V$  decrease for IM and LED events correlated on all PMTs.

Failure: PMT HV. Signature:  $Q$  and  $V$  change,  $Q/V$  constant on affected PMT correlated with variations on HVs for IM and LED events.

Failure: PMT window. Signature: Same as above but uncorrelated with HVs for IM and LED events.

Failure: Tank liner. Signature: Similar to dirty water, LED events show less variation depending on LED location.

Failure: Afterpulsing. Signature: D-P rate increases, correlated with peaks on  $t_{12}$ .

Failure: Ice. Signature: Water temperature.

Failure: Water leaks. Signature:  $Q$ ,  $V$  decrease on all PMTs correlated with water height.

Failure: PMT signal reflections, overshooting, rings, etc. Signature: Abnormal PMT traces, rates increase for D-P events. Transfer of the full PMT traces (500 ns for 4 ADCs at 10 bits/ADC and 25 ns sampling period gives 1 Kbit which can be transferred in about 5 s at 200 bit/s) can help elucidate the exact nature of the failure in these cases.

In addition, test leads will exist at each station to perform a more thorough diagnosis of its performance in situ.

### 3 Conclusions:

We have discussed one way in which the natural flux of background muons can be used to calibrate and monitor each of the 1600 WCDs of the Pierre Auger Observatory remotely. Two types of events can be used: crossing and decaying muons. The triggers to be used to collect the events from which the calibration and monitoring histograms can be obtained on-line have been listed. The calibration and monitoring procedures are similar to the ones described elsewhere (Alarcón et al., 1999) for a tank of reduced dimensions with a single PMT; in the case of full-sized WCDs with three PMTs the procedures have the additional advantage that the trigger can be defined to require double or triple coincidences of the PMT signals. A detailed list of the different diagnoses that can be performed on-line on the basis of the monitoring histograms was also discussed.

### References

- Alarcón, M. et al. 1999, Nucl. Instr. and Meths. in Phys. Res. A 420, 39  
Auger Collaboration 1997, "The Pierre Auger Project – Design Report",  
<http://www.auger.org/admin/DesignReport/index.html>  
Greisen, K. 1965, Phys. Rev. Lett. 16, 748  
Zatsepin, G.T. and Kuz'min, V.A. 1966, JETP Letters 4, 78